Contents

Chapter A

Example: Iterative homomorphic speckle reduction with a Wiener filter

In this chapter we give a complete example of parameter estimation taking into account the knowledge of the full image formation process. The example is for a class of images obtained in coherent illumination like laser, synthetic aperture radar (SAR), sonar, echography, computer tomography.

A.1   Image formation process

We consider the coherent imaging system presented in Fig. A.1. A rough surface (compared with the wavelength of the incident radiation) is illuminated by a unit-amplitude coherent field.

The reflectance of the surface $\xi = \xi(k,l)$ is the product of the object amplitude reflectance $x^{\frac{1}{2}} = x^{\frac{1}{2}}(k,l)$ and the random phase $\exp(j\,\Phi) = \exp(j\,(k,l))$. (k,l) are the spatial coordinates on the illuminated surface. The image formation system is composed by two lenses and an aperture spaced by the focal distance of the lenses (Fig. A.1). Such a system is equivalent with a low pass filter of bandwidth given by the size of the aperture. From the point of view of optics, in any location of the screen (the image plane) are coming incident waves reflected by a large number of independent scatterers of the illuminated surface. These waves have random phases and produce in the image plane random interferences, the *speckle* effect. The mathematical model of the image formation is shown in Fig. A.3. Where $h = h(k,l)$ is the coherent point spread function of the system (the aperture), $\gamma = \gamma(k,l)$ is the complex image and $y = y(k,l)$ is the speckle intensity in the observed image. Speckle is a deterministic phenomena, namely *interference*, but due to our lack of knowledge of the detailed structure of the imaged surface it is best described by its statistical properties. The speckle restoration problem is a signal estimation problem where we extract the signal component x from the "noisy" data y.
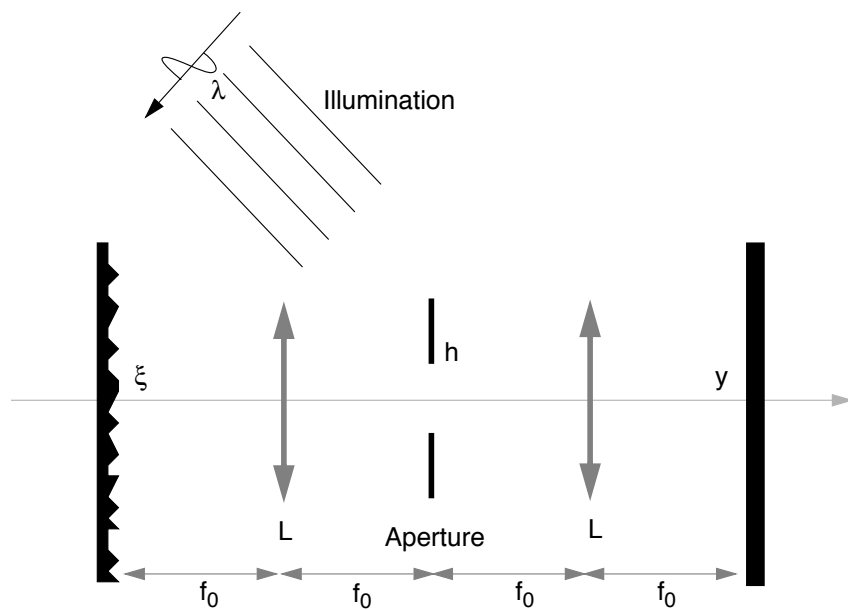
Figure A.1: Diagram of a typical coherent imaging system. The incident coherent radiation of wavelength λ is reflected by a rough surface of reflectance x. A system of 2 lenses and an aperture spaced by the focal distance have the effect of a direct Fourier transform, a low-pass filter, and an inverse Fourier transform. Thus the reflectance x is imaged in the plane y.
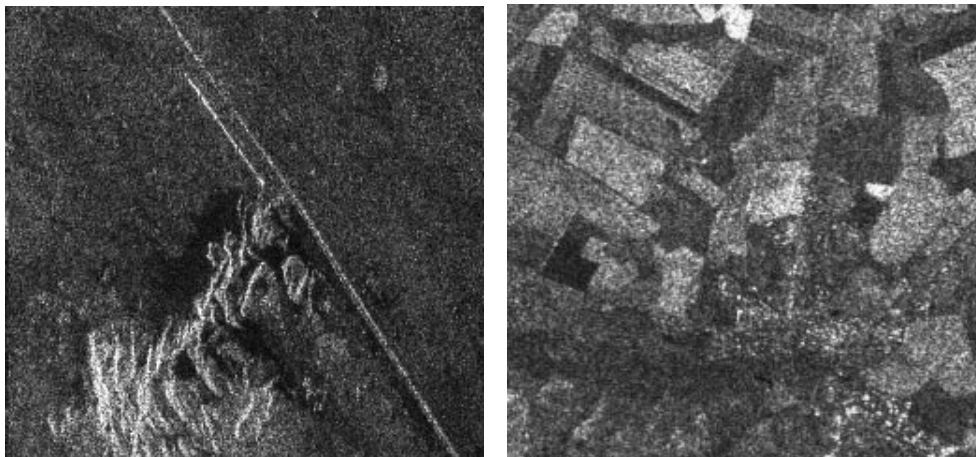
Figure A.2: Two examples of coherent images: Synthetic Aperture Radar. Left XSAR image "train", $\lambda = 3$cm, image resolution 12.5m. Right, ERS-1 image "agriculture, $\lambda = 5$cm, image resolution 20m. Both images have 512x512 pixels. The multiplicative nature of speckle can be observed when comparing the rough aspect of high reflectance regions with the smooth appearance of the dark areas.
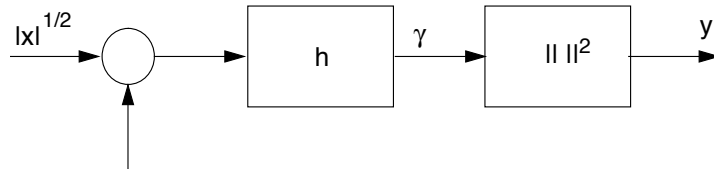
Figure A.3: Mathematical model of the coherent image formation. The intensity image y is obtained from the convolution of the complex reflectance with the filter h. The complex reflectance is represented its amplitude x and phase Φ.

A.2 Speckle statistics

In many practical applications, the object surface is extremely rough compared to the wavelength. This is called *fully developed speckle*. In this case the phase function Φ is an uncorrelated random field uniformly distributed between 0 and 2π. We also assume that Φ is statistically independent of the original image intensity x. Thus the scene surface can be modeled as a collection of a large number of independent random scatterers. In this case the discrete complex amplitude of the complex image γ can be written

$$\gamma(m,n) = \sum_{k}\sum_{l} h(m-k, n-l)\, |x|^{\frac{1}{2}}(k,l)\mathrm{e}^{j\,\Phi(k,l)} \tag{A.1}$$

which is the convolution with the point spread function h. The intensity of the speckled image is

$$y(m,n) = ||\gamma(m,n)||^2. \tag{A.2}$$

Based on these assumptions and using the central limit theorem we find that the process γ can be approximated by a complex circular Gaussian process. (Both, its real and imaginary part are Gaussian processes of zero mean and identical variance; see Section 7.2.6.) Consequently y has a negative exponential p.d.f. (cf. Section 7.2.5. where we apply the square function to transform a Rayleigh distributed r.v.).

$$p(y|x) = \frac{1}{x}\mathrm{e}^{-\frac{y}{x}}, \qquad y \geq 0 \tag{A.3}$$

$$p(y|x) = 0, \qquad y < 0 \tag{A.4}$$

Remark The p.d.f. $p(y|x)$ is the likelihood expressing the incertitude introduced by the noise, here the speckle process. We observe that speckle is a *multiplicative* noise.

$$y = x \cdot n \tag{A.5}$$

Thus the speckle noise is described by

$$\begin{aligned}
p(n) &= e^{-n}, & n \geq 0 & \qquad (A.6) \\
p(n) &= 0, & n < 0 & \qquad (A.7)
\end{aligned}$$

where $n = n(k, l)$.

A.3 The Covariance of the speckle image

The speckle image is obtained as the intensity of a circular complex Gaussian process.

$$n = ||\gamma||^2 \qquad \text{for } x = 1 \qquad (A.8)$$

Here we assume a rectangular aperture of size $\rho_k = \rho_l = \rho$, and using the Wiener-Khintchine theorem we obtain

$$C_n(k, l) = 1 + \text{sinc}^2 \frac{k}{\rho} \, \text{sinc}^2 \frac{l}{\rho} \qquad (A.9)$$

In the ergodic case the covariance is equal to the autocorrelation. We have now derived the likelihood model of the incertitude introduced by the speckle process. The model contains the statistical description of the speckle, the negative exponential p.d.f. and the deterministic image formation model given by the system point spread function h which is reflected in the autocorrelation function of the noise.

A.4 Homomorphic filtering of the multiplicative noise

The chosen image formation system was modeled as a system with multiplicative noise

$$y = x \cdot n \qquad (A.10)$$

Thus the homomorphic transform is a logarithmic one, so that the product is transformed in a sum. This new signal will be Wiener-filtered in order to obtain an estimate of the image intensity. Finally, the de-noised signal will be predicted, thus recovering the nature of the original input signal. The diagram in Fig. A.4 presents the homomorphic transform.

A.5 Statistical characterization of signal under the logarithmic transform

We investigate the statistics of speckle after a log transform. Using Eq. 7.40-7.44 for

$$f(\cdot) = \log(\cdot) \qquad (A.11)$$

we obtain the p.d.f. of the process

$$\begin{aligned}
n' &= \log n & \qquad (A.12) \\
p(n') &= \exp(n' - e^{-n'}) & \qquad (A.13)
\end{aligned}$$
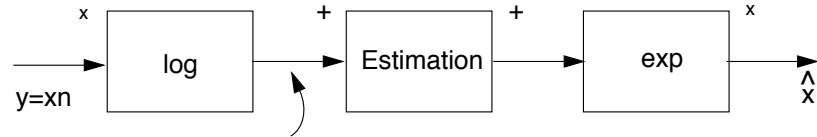
Figure A.4: Diagram of the homomorphic transform. The product $x \cdot n$ is transformed in the sum $\log(x) + \log(n)$. A linear estimator of $\log(x)$ is applied. The desired parameter x is recovered after exponentiation.

The new r.v. n' has the expectation

$$\mathcal{E}[n'] = \int_{-\infty}^{+\infty} n' p(n') \mathrm{d}n' = -\epsilon \tag{A.14}$$

where ϵ is the Euler constant. The design of the Wiener filter requires the knowledge of the covariance of the noise

$$R_{n'}(\triangle k, \triangle l) = \mathcal{E}[n'(k, l) \, n'(k + \triangle k, l + \triangle l)] \tag{A.15}$$

Using the shorthand notation $n_1 = n(k, l)$ and $n_2 = n'(k + \triangle k, l + \triangle l)$ the joint p.d.f. of the process n_1 and n_2 is

$$
p(n_1, n_2) = \frac{\exp\left[-\dfrac{n_1 + n_2}{\mathcal{E}[n] \, (1 - |\mu_n(\triangle k, \triangle l)|^2)}\right]}{\mathcal{E}[n]^2 \, (1 - |\mu_n(\triangle k, \triangle l)|^2)} \cdot
$$
$$
I_0\left(\frac{2 \, \sqrt{n_1 n_2} |\mu_n(\triangle k, \triangle l)|}{\mathcal{E}[n] \, (1 - |\mu_n(\triangle k, \triangle l)|^2)}\right) . \tag{A.16}
$$

I_0 is the modified Bessel function of first kind, and $\mu_n(\triangle k, \triangle l)$ is the correlation coefficient.

$$R_n(\triangle k, \triangle l) = \mathcal{E}[n]^2 \left(1 + |\mu_n(\triangle k, \triangle l)|^2\right) \tag{A.17}$$

It follows

$$R_{n'}(\triangle k, \triangle l) = \int_0^{+\infty} \int_0^{+\infty} \mathrm{d}n_1 \, \mathrm{d}n_2 \, \log n_1 \, \log n_2 \, p(n_1, n_2) \tag{A.18}$$

using the series expansion

$$I_0(\xi) = \sum_{k=0}^{\infty} \frac{\left(\frac{\xi}{2}\right)^{2k}}{(k!)^2} \tag{A.19}$$

and letting $\alpha = (1 - |\mu_n(\triangle k, \triangle l)|^2)$ we find

$$
\begin{aligned}
R_{n'}(\triangle k, \triangle l) &= \frac{1}{\alpha} \int_0^{+\infty} \int_0^{+\infty} dn_1 \, dn_2 \, \log n_1 \, \log n_2 \, \exp\left(-\frac{n_1 + n_2}{\alpha}\right) \cdot \\
&\quad \sum_{k=0}^{\infty} \frac{1}{(k!)^2} \left(\frac{n_1 n_2 \, |\mu_n|^2}{\alpha^2}\right)^k \quad\quad\quad\quad\quad\quad\quad (A.20)\\
&= \frac{1}{\alpha} \sum_{k=0}^{\infty} \frac{|\mu_n|^2}{(k!)^2 \alpha^{2k}} \int_0^{+\infty} dn_1 \, \log n_1 \, \exp\left(-\frac{n_1}{\alpha}\right) n_1^k \cdot \\
&\quad \int_0^{+\infty} dn_1 \, \log n_2 \, \exp\left(-\frac{n_2}{\alpha}\right) n_2^k \quad\quad\quad\quad\quad (A.21)\\
&= \alpha \sum_{k=0}^{\infty} |\mu_n|^{2k} \left[\sum_{i=1}^{k} \frac{1}{i} - \gamma + \log \alpha\right]^2 \quad\quad\quad\quad (A.22)
\end{aligned}
$$

Until now we specified the noise and image formation process in the covariance $C_{n'}$.

A.6   Wiener filter

The Wiener filter requires additional *prior* information, the model of the desired parameter x, expressed also as a covariance matrix C_x (Eq. 8.82). It is very seldom to have access to such knowledge, mainly dealing with images of unknown scenes or high complexity, i.e. different areas characterized by different covariance matrices. A possible solution is an iterative procedure. We consider an initial estimator of C_x. For example the covariances of the log of the observations $C_{y'}, y' = \log y$. This guess will be used to implement a first Wiener filter.

$$
x'^{(1)} = C_{x'}^{(0)} (C_{x'}^{(0)} + C_{n'})^{-1} y' \quad\quad\quad\quad (A.23)
$$

The estimated $x'^{(0)}$ will be further used to guess a new estimate of the covariance matrix $C_{x'}^{(0)}$, which at its turn will allow the implementation of a new filter. Thus in a generic iteration step k the estimate of the image will be

$$
x'^{(k+1)} = C_{x'}^{(k)} (C_{x'}^{(k)} + C_{n'})^{-1} y'. \quad\quad\quad\quad (A.24)
$$

The algorithm is convergent but at limit $k \to \infty$ does not exactly converge to the covariance of x'. There are methods to improve the estimation, but we do not address this here.

A.7   Conclusion

This example showed a complete image estimation problem recalling description of the physical process of imaging, its signal and system modeling and finally the stochastic analysis. The example addresses one of the common practical difficulties: The non-availability of the prior, which can be trained from the observations. This solution implicitly has as result the accommodation of the estimator to the non-stationarity of the signal.

Chapter 9

Gibbs-Markov random fields

We have seen that a stochastic process is fully determined by the knowledge of all p.d.f.s.

$$\lim_{n\to\infty} p(x(t_1),\ldots,x(t_n)) \tag{9.1}$$

where $x(t_k)$ is a r.v. obtained by sampling the process at the time t_k. As a reminder to the case of random images the time coordinate $\{t_k\}$ is substituted by the space coordinates $\{(k,l)\}$.

As presented in the previous chapters the success of image analysis depends on the accuracy and capacity to model images. Unfortunately learning high order p.d.f.s from training data is drastically limited by the large amount of data required. In this chapter we introduce a class of parametric models able to describe a large variety of image structures. This class has a high practical importance.

9.1   Markov stochastic processes

We use the following notation for the process:

$$p(x(t_1),\ldots,x(t_n)) = p(x_1,\ldots,x_n;\, t_1,\ldots,t_n). \tag{9.2}$$

Thus we make evidence of the states x_k, e.g. gray levels of an image and the time t_k evolution (the space coordinates in the case of images). A Markov process of first order is characterized by

$$p(x_n;t_n|x_1,\ldots,x_{n-1};t_1,\ldots,t_{n-1}) = p(x_n;t_n|x_{n-1};t_{n-1}). \tag{9.3}$$

The state of the process x_n at time t_n depends on its history only by the directly preceding state x_{n-1} at time t_{n-1}. (It was assumed $t_1 \leq \cdots \leq t_n$.) One can write

$$p(x_1,\ldots,x_n;\, t_1,\ldots,t_n) = p(x_1,\ldots,x_{n-1};t_1,\ldots,t_{n-1})\, p(x_n;t_n|x_{n-1};t_{n-1}) \tag{9.4}$$

$$p(x_1,\ldots,x_{n-1};\, t_1,\ldots,t_{n-1}) = p(x_1,\ldots,x_{n-2};t_1,\ldots,t_{n-2})\, p(x_{n-1};t_{n-1}|x_{n-2};t_{n-2}), \tag{9.5}$$

thus

$$p(x_1,\ldots,x_n;\, t_1,\ldots,t_n) = p(x_1;t_1) \prod_{k=2}^{n} p(x_k;t_k|x_{k-1};t_{k-1}), \tag{9.6}$$

where

$$p(x_1; t_1) = \int_{-\infty}^{+\infty} dx_2 \, p(x_1, x_2; t_1, t_2) \tag{9.7}$$

and

$$p(x_2; t_2 | x_1; t_1) = \frac{p(x_1, x_2; t_1, t_2)}{p(x_1; t_1)} \tag{9.8}$$

We conclude that a first order Markov process is characterized by the 2-dimensional joint p.d.f. For a stationary process

$$p(x_1, \ldots, x_n; \, t_1, \ldots, t_n) = p(x_1) \prod_{k=2}^{n} p(x_k; \triangle t_k | x_{k-1}). \tag{9.9}$$

with $\triangle t_k = t_k - t_{k-1}$. The process depends only on the time shift $\triangle t_k$.

9.2   Markov processes in 2 dimensions

Markov processes generalized to 2 dimensions are used to characterize spatial or contextual dependencies. The dependencies are defined locally in between neighborhood pixels but they characterize an entire image or extended region of an image.

9.2.1   Neighborhood and cliques

We introduce several topological notions. An image is considered to be defined as the pixel intensities in the nodes of a regular lattice $\mathcal{L}$. The sites in $\mathcal{L}$ are related to each other via a neighborhood system

$$\mathcal{N} = \{ \mathcal{N}_r \, | \forall r \in \mathcal{L} \}, \tag{9.10}$$

where $\mathcal{N}_r$ is the set of sites neighboring i. The vicinity relationship has the following properties:

1. A sites is not neighboring to itself $i \notin \mathcal{N}_i$.

2. The neighboring relationship is mutual:

$$r \in \mathcal{N}_s \leftrightarrow s \in \mathcal{N}_r$$

For a given site a nested neighborhood system is defined as depicted in Fig. 9.1. When the sites in a regular rectangular lattice $\mathcal{L} = \{(i,j) \, | 1 \leq i, j \leq N\}$ correspond to the pixels of an $N \times N$ image in the 2-dimensional plane, an internal site (i,j) has four nearest neighbors as $\mathcal{N}_{i,j} = \{(i-1,j), (i+1,j), (i,j-1), (i,j+1)\}$. The pair $(\mathcal{L}, \mathcal{N}) = \mathcal{G}$ is a graph, where $\mathcal{L}$ contains the nodes and $\mathcal{N}$ specifies the links according to the vicinity relationships. A *clique* c for $\mathcal{G}$ is defined as a subset of sites in $\mathcal{L}$, an example is presented in Fig. 9.1. The sites in a clique are ordered, $\{i, j\}$ is not the same clique as $\{j, i\}$. The type of a clique is determined by its size, shape and orientation.
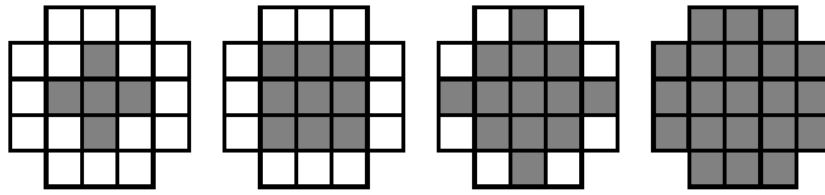
Figure 9.1: Nested system of neighborhood, order I to IV.

9.2.2 Markov random fields (MRF)

A random image X as a realization of a stochastic process, defined on a lattice $\mathcal{L}$, is also called a *random field*. A Markov random field (MRF) is defined on a lattice $\mathcal{L}$ with respect to a neighborhood system $\mathcal{N}$ if and only if

$$p(x) > 0 \tag{9.11}$$
$$p(x_s|x_r; r \neq s) \;=\; p(x_s|x_r; r \in \mathcal{N}_s) \tag{9.12}$$

where s and r are two sites in $\mathcal{L}$. Only neighboring pixels have direct interaction. The Markovianity is a *local* characterization of the random field.

9.2.3 Gibbs random fields (GRF)

Table 1: Graphical definition of GRFs

NEIGHBOR-HOOD	$\mathcal{N}^I$			$\mathcal{N}^{II}$			
CLIQUES	▪	▯ ▭	▪	▯ ▭	◿◺	◰◱◲	▦
PARAMETERS	α_0	α_1 α_2	α_0	α_1 α_2 α_3 α_4	β_1 β_2 β_3 β_4		γ_0
POTENTIAL	V_1^1	$V_2^1 V_2^2$	V_1^1	$V_2^1 V_2^2 V_2^3 V_2^4$	$V_3^1 V_3^2 V_3^3 V_3^4$		V_4^1
ENERGY	U^I		U^{II}				

NOTE: $\alpha_0, \dots \alpha_4$, $\beta_1, \dots \beta_4$, γ_0, are the model parameters associated to the corresponding cliques, V is the potential function characterizing the interaction between the samples of the random field inside the clique (the subscript is the order of the clique and the superscript refers to the clique index), U is the energy function for the corresponding neighborhood (the superscript is the order of the neighborhood).

A random field is said to be a Gibbs random field (GRF) in $\mathcal{L}$ with respect to $\mathcal{N}$ if

and only if its configurations are characterized by a Gibbs distribution

$$p(x) = \frac{1}{Z} e^{-\frac{1}{T} U(x)} \tag{9.13}$$

where Z is the partition function

$$Z = \int \mathrm{d}x \, p(x) \tag{9.14}$$

T is a constant called *temperature* and $U(x)$ is an energy function

$$U(x) = \sum_{c \in \mathcal{C}} V_c(x) \tag{9.15}$$

defined as the sum of the potential functions $V_c(x)$ over the set of all cliques $\mathcal{C}$. For example a Gaussian is a Gibbs distribution. The Gibbs distribution $p(x)$ measures the probability of a particular configuration (structure) in the random image X. The more probable configurations are those with lower energies. The temperature T controls the sharpness of the distribution (in a similar way to the variance in a Gaussian distribution). At high temperatures all configurations tend to be equally distributed.

The potential function $V_c(x)$ describe in a parametric manner the type of interactions in between the pixels in a clique. Thus characterizing the structural patterns in the image. Given the type of potential function one obtains all the information about the random field by estimation of this parameters from the observed data.

9.2.4 Markov-Gibbs equivalence

MRF are interesting due to their local characterization, however they result in complex computations and difficulties in consistent definition.

GRF are characterized by global properties. The *Hammersley-Clifford* theorem establishes the equivalence of these two types of properties. The theorem states that a random field is a MRF in $\mathcal{L}$ with respect to $\mathcal{N}$ if and only if it is a GRF in $\mathcal{L}$ with respect to $\mathcal{N}$. This equivalence provides us with a simple and practical way of specifying a MRF by using potential functions instead of local characteristics (which is usually impossible) consider

$$p(x_s | x_r; r \neq s) = \frac{e^{-\frac{1}{T} \sum_{c \in \mathcal{C}} V_c(x)}}{\sum_\xi e^{-\frac{1}{T} \sum_{c \in \mathcal{C}} V_c(\xi)}} \tag{9.16}$$

where $\xi = \{x_r | r \neq s\}$ is any configuration which agrees with X at all sites except s.

We divide now the set of all cliques $\mathcal{C}$ in two sets $\mathcal{A}$ and $\mathcal{B}$. $\mathcal{A}$ consists of cliques containing s and $\mathcal{B}$ of cliques not containing s. Thus we have

$$p(x_s | x_r; r \neq s) = \frac{\exp\left(-\frac{1}{T} \sum_{c \in \mathcal{A}} V_c(x)\right) \exp\left(-\frac{1}{T} \sum_{c \in \mathcal{B}} V_c(x)\right)}{\sum_\xi \exp\left(-\frac{1}{T} \sum_{c \in \mathcal{A}} V_c(\xi)\right) \exp\left(-\frac{1}{T} \sum_{c \in \mathcal{B}} V_c(\xi)\right)}. \tag{9.17}$$

Because $V_c(x) = V_c(\xi)$ for any clique c that does not contain s, the factors

$$\exp\left(-\frac{1}{T} \sum_{c \in \mathcal{B}} V_c(x)\right) \text{ and } \exp\left(-\frac{1}{T} \sum_{c \in \mathcal{B}} V_c(\xi)\right) \tag{9.18}$$

cancel. It result

$$p(x_s|x_r; r \neq s) = \frac{\exp\left(-\frac{1}{T}\sum_{c \in \mathcal{A}} V_c(x)\right)}{\sum_{\xi} \exp\left(-\frac{1}{T}\sum_{c \in \mathcal{A}} V_c(\xi)\right)} \tag{9.19}$$

which depends only on the neighbors of s,thus

$$p(x_s|x_r; r \neq s) = p(x_s|x_r; r \in \mathcal{N}_s). \tag{9.20}$$

That is demonstrating the equivalence of GRFs and MRFs. The full proof of equivalence is too complex to be given here.